magnetic properties of the impurities. It should be noted, however, that the values for the intrinsic relaxation rate $(1/T_{dl})$ of the magnetic impurities differ by an order of magnitude for Mn and Cr and by two orders of magnitude for Fe.[38]

VI. CONCLUSION

In conclusion, we summarize briefly the experimental results of this work and their possible theoretical implications: The observation of TESR in dilute Cu-Cr alloys strongly suggests the feasibility of analogous studies on other systems. These include both transition and rare-earth metallic impurities in different metals. From the analysis of the signal behavior as a function of temperature and concentration, a very good fit is made to the phenomenological model of Hasegawa (suitably modified). From this fit the intrinsic g value of Cr, the intrinsic relaxation rate of Cr, and its spin scattering cross section are deduced along with a determination of the spin susceptibility of pure copper. This determination throws some insight on the Fermi-liquid behavior of the electrons of the host metal.

The main questions raised by these results are: Why is the g factor of Cr so near the free-electron value? What is the strong mechanism responsible for the intrinsic relaxation rate $(1/T_{dl})$ of Cr, and why is it temperature-independent? Why is the Kondo scattering phenomena apparently absent from the dynamic behavior of this spin system down to a temperature close to the Kondo temperature?

[38] From Ref. 11; T_{dl} for Mn is 2.9×10^{-9} sec, our value for Cr is 5×10^{-10} sec, and our preliminary value for Fe is $\sim5\times10^{-12}$ sec.

ACKNOWLEDGMENTS

We want to express our thanks to L. Creveling for performing the measurement of the static susceptibilities. We thank Dominique Jérome for neutron-activation analysis of the samples and Professor M. N. A. Peterson for generously helping with our chemical analysis. We are grateful to M. R. Shanabarger and Dr. Y. Yafet for many helpful discussions.

PHYSICAL REVIEW VOLUME 173, NUMBER 3 15 SEPTEMBER 1968

Lattice-Dynamical Properties of Fe^{57} Impurity Atoms in Pt, Pd, and Cu from Precision Measurements of Mössbauer Fractions*

RUDI H. NUSSBAUM, DONALD G. HOWARD, WILBUR L. NEES, AND CHARLES F. STEEN
Portland State College, Portland, Oregon 97207

(Received 25 April 1968; revised manuscript received 6 June 1968)

Precision measurements of the Mössbauer fractions of Fe^{57} in single crystals of Cu, Pd, and Pt were obtained over a range from liquid-helium temperatures to around 750°K in about 50°K intervals, using the "black wide absorber" technique. The over-all accuracy is estimated to be better than 0.7%, with a somewhat larger error for Pt. Our data are consistent with a harmonic lattice with small cubic and quartic anharmonic contributions. Properly weighted Debye temperatures $\Theta_D(-1)$ and $\Theta_D(-2)$ were derived from the low- and high-temperature limits of our f measurements, which were compared with equivalent data for the pure hosts. We conclude that Fe in Cu is about 20% more strongly bound than Cu in Cu, while Fe in Pd and Pt shows about a 20% weaker average force constant than the host atoms. Fe in Cu also has a much larger degree of anharmonicity than pure Cu. Analysis of earlier data on Fe in Ni shows a similar behavior. Our data were also examined for evidence of localized impurity modes. The low-temperature data for Fe in Pt are consistent with the existence of a predicted localized mode, but they do not provide unambiguous evidence.

1. INTRODUCTION

THE probability for the emission of γ rays from radioactive atoms without energy exchange with the lattice vibrations of the crystal in which they are embedded (the Mössbauer effect) depends upon the strength of the interatomic forces between these atoms and the crystal. Precision measurements of the temperature-dependent Mössbauer fraction f (also known as the Debye-Waller factor) yield the temperature dependence of the mean-squared displacement of the emitting nucleus[1] $f(T)=\exp(-\kappa^2\langle x^2\rangle_T)$, where κ is the wave number of the Mössbauer γ ray. In particular, if the Mössbauer atoms are dilute impurities in pure host materials, such measurements may yield rather unique information of the impurity-to-host binding relative to the host-to-host binding, provided that similar lattice dynamical data for the host material are available for comparison.[1] If measurements of the Mössbauer fraction f are obtained over a range from liquid-helium temperatures to temperatures sufficiently high that classical equipartition of the energy can be expected to hold, the data can be interpreted in terms of the high- and low-temperature

* Work supported by a National Science Foundation Research Grant.

[1] A thorough discussion of the analysis of Debye-Waller factors in terms of lattice dynamics of harmonic crystals is given by R. M. Housley and F. Hess, Phys. Rev. 146, 517 (1966). The reader will find earlier references there.

limits of harmonic-lattice-dynamical models,[1] provided that the data in the medium-to-high temperature range are accurate enough to take properly into account the effects of cubic and quartic anharmonicity[2,3] which become increasingly important at high temperatures.

Low-temperature f measurements in some substances have revealed, in addition, large deviations in $\langle x^2\rangle_T$ from the behavior predicted by harmonic models.[4] Such anomalies may be due either to strongly anharmonic interatomic forces or to the slow relaxation of highly excited localized vibrational modes.[5] Localized modes have been theoretically predicted for certain ranges of impurity-host mass ratios and/or force-constant changes for certain simplified models.[2,6,7] Their existence has been confirmed in a number of materials by neutron scattering and optical techniques.

The required accuracy for meaningful lattice-dynamical analysis of experimental values of $\langle x^2\rangle_T$ is very high. The "wide black" absorber techniques for Fe^{57} Mössbauer radiation[8] make absolute measurements of f possible to a precision of a few tenths of a percent. This technique has been employed in the present series of experiments, which were intended to reinvestigate the previously reported apparent anomalous decrease in f below that which might be predicted from a harmonic-crystal model for Fe^{57} substitutional impurities in a number of cubic-metal hosts[9] at very low as well as at high temperatures. As part of a series of studies of Fe^{57} impurities in cubic-metal hosts of varying masses and interatomic spacing, we have measured the Mössbauer fraction of Fe^{57} in high-purity single crystals of palladium and platinum from about 10°K to about 750°K, and in a high-purity copper crystal above about 100°K. The over-all accuracy of our data is estimated to better than 0.7%.

This paper is divided into three major sections. In Sec. 2, we discuss in detail the experimental techniques used to obtain the raw data, as well as the important corrections affecting the accuracy of the final f values. In Sec. 3, we outline the theory and methods used to reduce our data in terms of lattice-dynamical parameters; we also compare the parameters obtained for the Fe impurities with those for the pure host materials. We have included here a discussion of earlier data on Fe and Ni. Finally, in Sec. 4, the major conclusions from this comparison are discussed: The Fe impurities are more tightly bound in Cu and Ni than are the host atoms, while the opposite is true for the binding of Fe in Pd and Pt. These results are correlated with the sign of the changes in lattice spacings on alloying Fe with these four hosts. The data are also examined for information on impurity anharmonicity, as well as on evidence for localized impurity modes.

2. EXPERIMENTS

2.1 Sample Preparation

Small disks of about 3–5 mm diam by 2 mm thick were cut from 99.995%-purity single-crystal chips of Pd, Pt, and Cu. Approximately $\frac{1}{3}$ mCi of high-specific-activity $Co^{57}Cl_2$ in HCl was pipetted onto carefully cleaned surfaces on which a deposit of beef albumen served as wetting agent. Each sample was then individually heated to 500°C in H_2, flushed with purified He, and diffused in low-pressure He ($\approx 10^{-4}$ Torr), the Pt and Pd at 1000°C for 20 min and the Cu at 900°C for 45 min. Surface activity was removed by scrubbing with pumice soap and water.

For each source, a γ-ray energy spectrum was taken, using a Xe-CH_4-filled proportional counter, an FET preamplifier, and a 512-channel pulse-height analyzer. All sources showed a well-resolved 14.4-keV energy peak, with the exception of the Pt source, where a small fraction of fluorescent Pt L x rays contribute to the 14.4-keV intensity as is shown in Fig. 1. From the relative intensities of the Pt L x rays[10] we estimate that the contribution of the L-γ_1 x ray to the 14.4-keV counting channel is not more than 1%. (see Sec. 2.3).

Resonance-line-shape measurements (on our sources) using a thin natural-Fe absorber have yielded the following widths at half-maximum: Cu: 0.20±0.01 mm/sec; Pd: 0.21±0.01 mm/sec; Pt: 0.21±0.01 mm/sec. After additional diffusion of the Pd and Pt sources (see Sec. 3.1), the relative intensities of the x rays were greatly enhanced, indicating a considerable penetration of the activity into the bulk material. However, the Mössbauer linewidths remained unaffected by the rediffusion.

2.2 Measuring Techniques

Measurements of the zero-phonon fraction f were made with the "black wide" absorber[11] mounted to a double-loudspeaker drive assembly using a balsa-wood frame, as shown schematically in Fig. 2. The sample was mounted in the appropriate equipment for varying and maintaining temperature, and was kept at rest with respect to the speakers. Above room temperature up to a maximum of about 450°C, the sample was mounted in a small vacuum furnace, consisting of an anodized aluminum block with heater winding, suppor-

[2] A. A. Maradudin and P. F. Flinn, Phys. Rev. **129**, 2529 (1963).
[3] K. N. Pathak and B. Deo, Physica **35**, 167 (1967).
[4] J. G. Dash, D. P. Johnson, and W. M. Visscher, Phys. Rev. **168**, 1087 (1968).
[5] J. G. Dash and R. H. Nussbaum, Phys. Rev. Letters **16**, 567 (1966); in *Proceedings of the Fourteenth Colloque Ampère (Atomes et Molécules par des Etudes Radio-Electriques), Ljubljana, 1966* (North-Holland Publishing Co., Amsterdam, 1967).
[6] W. M. Visscher, Phys. Rev. **129**, 28 (1963).
[7] G. W. Lehman and R. E. DeWames, Phys. Rev. **131**, 1008 (1963). Our $G_i(\omega)d\omega$ is identical with the normal-mode amplitudes b_{jik}^2 in Ref. 1 and the function $K(x,\epsilon)dx$ in the above article.
[8] R. M. Housley, N. E. Erickson, and J. G. Dash, Nucl. Instr. Methods **27**, 29 (1964).
[9] W. A. Steyert and R. D. Taylor, Phys. Rev. **134**, A716 (1964).
[10] *Nuclear Spectroscopy* (Academic Press Inc., New York, 1960), p. 218.
[11] This absorber was kindly loaned to us by R. D. Taylor at the Los Alamos Scientific Laboratory.

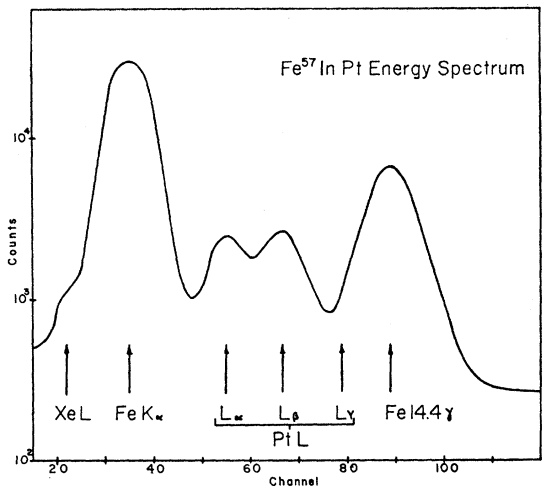

FIG. 1. Pulse-height spectrum of γ radiation from Co^{57}, diffused into Pt, taken with a Xe-CH_4-filled proportional counter.

ted axially by a ceramic post from a brass vacuum jacket. The radiation was emitted axially through a beryllium window in the vacuum jacket. Aluminum-foil heat shielding served to improve the thermal isolation. Below room temperature down to about 4°K, the sources were mounted in a variable-temperature cryostat[12] which employed a heat switch and a heater. The radiation axis was horizontal. Radiation emerged through a stack of aluminized Mylar heat shields and through a beryllium window in the vacuum jacket.

Above 50°K, temperatures were measured using a chromel-alumel thermocouple in contact with the sample. Below 50°K, the resistance of a composition resistor in contact with the sample holder was measured using a low-power ac bridge circuit.

2.3 Corrections to Data

It has been pointed out by Housley[13] that a number of corrections have to be made to the observed count rate in the 14.4-keV channel because of several different secondary scattering effects. The precision with which these can be determined governs the ultimate accuracy of precision f measurements. We have therefore listed below in detail what these corrections are, as well as how they were determined in our experiments.

The corrected zero-phonon fraction was calculated from the relation

$$f_{\text{corr}}=\frac{\beta I_\infty - I_0}{\beta I_\infty - \delta I_B}\,\frac{1}{C_B}\,\frac{1}{C_g}\,\frac{1}{C_c}\,\frac{1}{C_w}.$$

The meaning of these constants and the means for their evaluation are discussed below.

[12] D. P. Johnson, thesis, University of Washington, Seattle, 1967 (unpublished). These measurements were done at the University of Washington through the kind cooperation of J. G. Dash.
[13] R. M. Housley, Nucl. Instr. Methods 35, 77 (1965).

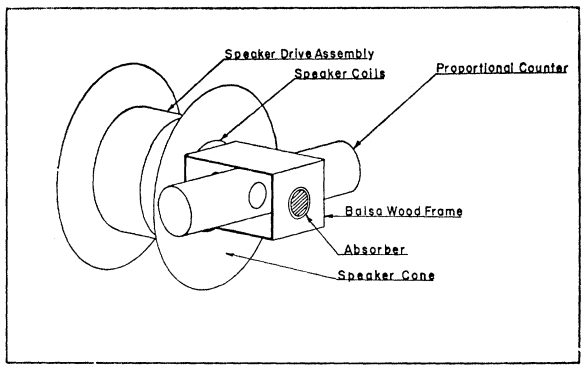

FIG. 2. Double-speaker drive and geometry of absorber and detector for f measurements and Mössbauer resonance spectra.

I_0: the resonance count rate at emission-absorption-line overlap, for which the relative velocity of the absorber is zero.

I_∞: the off-resonance count rate for a large swing in velocity ("buzzing"). This is accomplished by driving the speaker at 60 Hz such that the maximum velocity is of the order of 10 cm/sec.

β: the correction (1.008) for the finite time spent at resonance overlap while "buzzing."

I_B: the background count rate due to high-energy radiation, as measured with a 66-mg/cm^2 pure-copper foil inserted in the beam between source and absorber. The measured background for all sources was generally less than 10% of I_∞.

δ: the correction (1.02) to the background due to the transmission of the copper foil, which is 0.4% for the 14.4-keV and 98% for the 122-keV radiation from Fe^{57}.

C_B: the correction for the transmission of resonant radiation through the wide absorber, which is estimated to be (97.0±0.5)% opaque to zero-phonon 14.4-keV radiation. The transmission through the center of the wide resonance absorption line has been measured to be about 0.5% by superimposing a second wide absorber of approximately the same opacity and determining the increase in the measured f. To this correction must be added the fraction of the Mössbauer emission line from the source whose energy does not fall within the practically opaque part of the absorption line. Assuming that the emission line is Lorentzian (this assumption is supported by our measured linewidths; see Sec. 2.1), and adopting a simplified shape for the "tails" of the non-Lorentzian absorption spectrum of the wide absorber, Sprague[14] calculated the transmission through these "tails" to be about 2.5% of the total zero-phonon intensity. The uncertainty in this correction can only be estimated to be about 0.5%, and comprises a major source of possible systematic error in our measurements.

$1-C_g$: a correction for reradiation from the absorber into the detector, including Compton as well as resonant

[14] D. L. Sprague, thesis, University of Washington, Seattle, 1967 (unpublished).

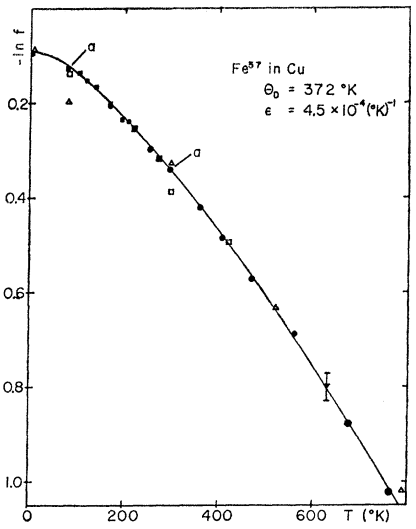

FIG. 3. Debye-Waller factor f of Fe^{57} in single-crystal Cu. The solid line is a Debye function, corrected for anharmonicity. (See Sec. 3.2.) (The size of the solid symbols represents statistical error in $-\ln f$.) □, Ref. 19; △, Ref. 9; *a*, Ref. 18; ▼, Ref. 17; ■, Ref. 14; ●, present work.

scattering. It ranges in our experiments from 0.2 to 0.8%, depending on geometry. (This is the constant k of Housley.[13])

$I-C_c$: a correction for Compton scattering in the source, including an upper bound for thermal diffuse scattering in the source, as discussed by Housley.[13] We assume for this purpose that the activity is concentrated in a thin layer near the surface of the source.[15] In the worst case (Pd), the scattering cross sections are such that the correction is less than 0.1% over our temperature range. For Cu and Pt, it is at least another factor of 3 less. This correction could therefore be neglected.

$I-C_w$: the correction for Compton scattering from the radiation windows, mainly those of beryllium. Like C_a, it has been calculated from the known geometry of each experimental setup[13]; it ranges from 0 to 4%. Since the effective geometry for the windows is often fairly uncertain, and since this correction also depends upon estimates of the Compton cross sections, we decided to determine this constant experimentally for the two geometries (furnace and cryostat) in the following manner: Numerous measurements of the room-temperature value of f were made for each source over a period of time and for each geometrical arrangement used. A careful measurement was also made for each source in a geometry without windows, for which $C_w=1$. By comparing all the f data for which $C_w=1$ with those measured in furnace and cryostat geometries, we obtained empirical values for C_w, independent of the sources used. Applying these correction factors, the resulting room-temperature f values for each source were found to be internally consistent to within the statistical accuracy of the individual measurements, which was better than 0.5%. Therefore, in evaluating the data at other temperatures, an empirical value of the correction C_w was used, as determined for each geometry at room temperature, from a comparison with the measurements for which $C_w=1$. This procedure improved the over-all accuracy of our data.

The possibility of self-absorption in the sample was investigated by measuring, in the absence of an absorber, the change in count rate if a field of about 9 kOe was applied around the source. The two count rates agreed to better than 0.01%, which was well within statistics.

An additional $(1\pm0.5)\%$ correction had to be made for the Pt sample to compensate for the unresolved L-γ_1 x ray, whose relative intensity is only known approximately.[16]

3. EXPERIMENTAL RESULTS

3.1 Data Reduction

Our values for $(-\ln f)=\kappa^2\langle x^2\rangle_T$, after applying the corrections discussed in Sec. 2.3, are shown plotted for each source in Figs. 3–5, together with values obtained by other investigators.[8,9,14,17–20] Our data are also given

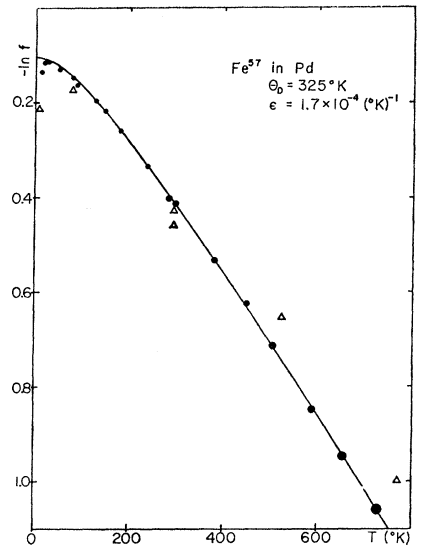

FIG. 4. Debye-Waller factor f of Fe^{57} in single-crystal Pd. The solid line is a Debye function, corrected for anharmonicity. (See Sec. 3.2.) (The size of the solid symbols represents statistical error in $-\ln f$.) △, Ref. 9; ●, present work.

[15] This assumption was supported by observing the relative intensities of the 14.4-keV radiation, the Fe x rays and the fluorescent x rays from the host; see Fig. 1.

[16] This estimate was made by a combination of the low-energy γ-ray spectra of our Pt source with the proportional counter (see Fig. 1) and a Si(Li) spectrometer, and the spectrum of an Au^{195} source. L x-ray intensity ratios are poorly known and estimates had to be made of the penetration absorption of these lines produced by fluorescence in our Pt source.

[17] D. G. Howard and J. G. Dash, J. Appl. Phys. **38**, 991(1967).

[18] R. M. Housley, J. G. Dash, and R. H. Nussbaum, Phys. Rev. **136**, A464 (1964).

[19] J. P. Schiffer, P. N. Parks, and J. Heberle, Phys. Rev. **133**, A1553 (1964).

[20] W. Kerler and W. Neuwirth, Z. Physik **167**, 194 (1962).

in Tables I–III. The indicated errors represent statistical uncertainty only, and therefore reflect internal consistency. Additional systematic errors (estimated to be about 0.5%) will further influence the absolute accuracy of the results as discussed in Sec. 2.3. The solid curves shown in the graphs have been calculated from a Debye model corrected for the effects of cubic and quartic anharmonicity, as discussed in Sec. 3.2.

For both the Pd and Pt source at our lowest temperatures, a slight decrease in f is apparent. It is well known that dilute solutions of Fe in Pd and Pt show ferromagnetic ordering at very low temperatures. Near the transition temperature the Mössbauer line will split up because of magnetic hyperfine structure, and a portion of the recoil-free intensity will fall outside of the absorption line of the wide absorber, thus effectively decreasing the observed resonance fraction. In order to distinguish between a true decrease of f and the onset of magnetic splitting, these two sources were diffused again for approximately 4h under the conditions already described in Sec. 2.1. Following rediffusion, both sources showed a large proportional decrease in the 14.4-keV intensity relative to the high-energy background and x-ray radiations, indicating that the activity was distributed over a considerably deeper layer of the samples, thus reducing the average Fe concentration. No decrease in the measured f was detected in the rediffused sources down to a temperature of 4°K, indicating a lowering of the magnetic transition temperature. Because of the increase in background and decrease in count rate caused by the rediffusion, however, the accuracy of these later f measurements was several times worse than the values obtained in the first low-temperature measurements. We have therefore not included the later values in our analysis.

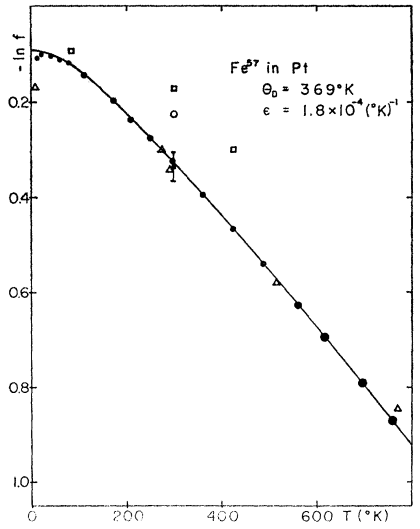

FIG. 5. Debye-Waller factor f of Fe^{57} in single-crystal Pt. The solid line is a Debye function, corrected for anharmonicity. (See Sec. 3.2.) (The size of the solid symbols represents statistical error in $-\ln f$.) ○, Ref. 20; □, Ref. 19; ■, Ref. 8; △, Ref. 9; ●, present work.

3.2 Derived Lattice-Dynamical Parameters

For harmonically bound crystals, the mean-squared displacement of the radiating atom is related to the phonon-frequency spectrum $G_h(\omega)$ in a monatomic crystal,[21] while for an impurity atom, $G_i(\omega)$ stands for the "dynamic-response function"[7] which describes the coup-

TABLE I. Debye-Waller factor and effective Debye temperatures Θ_D for Fe^{57} in Cu.

T (°K)	$\frac{\beta I_\infty - I_0}{\beta I_\infty - \delta I_B}$	f (corrected)	Θ_D (°K), assuming $\epsilon=4\times10^{-4}$	$\epsilon=4.5\times10^{-4}$	$\epsilon=5\times10^{-4}$ °K^{-1}
4	···	0.910±0.002[a]	363	363	363
79	···	0.882±0.002[a]	363	364	365
104	···	0.871±0.002[a]	376	378	379
119½±½	0.796	0.857±0.003	369	371	372
138	···	0.846±0.002[a]	377	378	379
170±½	0.757	0.814±0.003	367	369	371
170	···	0.817±0.002[a]	371	373	374
194	···	0.790±0.002[a]	364	365	367
207±½	0.731	0.786±0.002	371	373	375
220	···	0.772±0.002[a]	368	369	371
254±½	0.690	0.743±0.003	369	371	373
273	···	0.728±0.002[a]	370	372	374
295	···	0.709±0.002[a]	369	372	375
296±½	0.687	0.711±0.003			
296±½	0.660	0.710±0.003	371	374	377
296±½	0.667	0.709±0.003			
359½±½	0.617	0.656±0.003	369	372	374
406½±½	0.579	0.616±0.003	369	372	375
471±½	0.530	0.564±0.003	368	371	375
560±1	0.472	0.502±0.003	370	375	379
676½±1	0.390	0.415±0.003	367	371	376
764±2	0.338	0.359±0.003	365	371	377
		Mean Θ_D above 100°:	369.4±3.2	372.0±3.0	374.6±3.1

[a] Data from Ref. 14.

[21] G. K. Wertheim, *Mössbauer Effect* (Academic Press Inc., New York, 1964).

TABLE II. Debye-Waller factor and effective Debye temperatures Θ_D for Fe^{57} in Pd.

T (°K)	$\frac{\beta I_\infty - I_0}{\beta I_\infty - \delta I_B}$	f (corrected)	Θ_D (°K), assuming $\epsilon = 1\times10^{-4}$	$\epsilon = 1.5\times10^{-4}$	$\epsilon = 2\times10^{-4}$ °K^{-1}
$13\pm\frac{1}{2}$	0.842	0.875±0.002			
$19\pm\frac{1}{2}$	0.857	0.891±0.002	304	304	304
$24\frac{1}{2}\pm\frac{1}{2}$	0.858	0.891±0.002	310	310	310
$50\pm\frac{1}{2}$	0.844	0.877±0.002	308	308	308
$78\pm\frac{1}{2}$	0.830	0.863±0.002	321	321	322
88±1	0.818	0.850±0.002	312	313	314
$126\pm\frac{1}{2}$	0.764	0.823±0.003	323	325	326
147±1	0.747	0.804±0.003	325	326	327
180±1	0.716	0.771±0.003	323	324	326
236±2	0.664	0.715±0.003	321	323	325
282±1	0.644	0.669±0.003	319	321	323
$295\pm\frac{1}{2}$	0.639	0.662±0.003			
$295\pm\frac{1}{2}$	0.621	0.661±0.003	321	323	326
$295\pm\frac{1}{2}$	0.614	0.660±0.003			
$295\pm\frac{1}{2}$	0.634	0.659±0.003			
$380\pm\frac{1}{2}$	0.552	0.587±0.003	321	324	326
$448\frac{1}{2}\pm1$	0.503	0.535±0.003	322	326	329
505±1	0.462	0.491±0.003	321	325	328
589±2	0.403	0.428±0.003	317	322	326
655±2	0.364	0.387±0.003	318	322	328
727±2	0.326	0.347±0.003	318	324	329
		Mean Θ_D above 100°:	320.8±2.4	323.8±1.6	326.6±1.8

TABLE III. Debye-Waller factor and effective Debye temperatures of Fe^{57} in Pt.

T (°K)	$\frac{\beta I_\infty - I_0}{\beta I_\infty - \delta I_B}$	f (corrected)	Θ_D (°K), assuming $\epsilon = 1.5\times10^{-4}$	$\epsilon = 1.75\times10^{-4}$	$\epsilon = 2.0\times10^{-4}$ °K^{-1}
11.8±0.3	0.855	0.897±0.003	...	...	...
$20\pm\frac{1}{2}$	0.862	0.905±0.003	350	350	350
$40\pm\frac{1}{2}$	0.859	0.902±0.003	360	361	363
$59\pm\frac{1}{2}$	0.853	0.895±0.003	360	361	363
$78\pm\frac{1}{2}$	0.848	0.890±0.004	375	376	377
$110\pm\frac{1}{2}$	0.797	0.866±0.004	368	369	370
$171\pm\frac{1}{2}$	0.756	0.821±0.004	369	370	371
$209\pm\frac{1}{2}$	0.726	0.789±0.004	366	367	368
$249\pm\frac{1}{2}$	0.698	0.759±0.004	368	369	370
$295\pm\frac{1}{2}$	0.673	0.723±0.004			
$295\pm\frac{1}{2}$	0.692	0.723±0.004	368	369	370
$295\pm\frac{1}{2}$	0.669	0.727±0.004			
$365\pm\frac{1}{2}$	0.627	0.674±0.004	369	371	373
$424\pm\frac{1}{2}$	0.584	0.627±0.004	366	368	370
$488\frac{1}{2}\pm\frac{1}{2}$	0.544	0.583±0.004	366	368	370
560±1	0.498	0.534±0.004	366	368	370
617±1	0.464	0.499±0.004	365	368	370
696±1	0.422	0.453±0.004	365	368	371
$760\frac{1}{2}\pm\frac{1}{2}$	0.390	0.419±0.004	366	369	372
		Mean Θ_D above 80°K:	367±1.5	368.5±1.0	370.5±1.2

ling of the impurity modes to the unperturbed normal modes of the host [in that case, $G_i(\omega)$ also depends on the impurity-host mass ratio and may include localized vibrational modes[7]]:

$$\langle x^2\rangle_T = \frac{\hbar}{m}\int_0^\infty \left[\frac{1}{2}+\frac{1}{e^{\hbar\omega/kT}-1}\right]\frac{G(\omega)}{\omega}d\omega$$

$$= \frac{\hbar}{2m}\int_0^\infty \coth\left(\frac{\hbar\omega}{2kT}\right)\frac{G(\omega)}{\omega}d\omega, \quad (1)$$

where $G(\omega)$ is assumed to be normalized, $\int_0^\infty G(\omega)d\omega = 1$.

At very low temperatures, the zero-point motion dominates $\langle x^2\rangle_T$, and from Eq. (1) for $T\rightarrow 0$°K

$$\langle x^2\rangle_0 = \frac{\hbar}{2m}\int_0^\infty \frac{G(\omega)}{\omega}d\omega. \quad (2)$$

This limit is reached in most practical cases at liquid-He temperatures.[1]

At high temperatures ($\hbar\omega_{\max}/kT < 2\pi$), $\coth(\hbar\omega/2kT)$

in Eq. (1) can be expanded[1]:

$$\langle x^2\rangle_T=\frac{kT}{m}\int_0^\infty\left[1+\tfrac{1}{12}\left(\frac{\hbar\omega}{kT}\right)^2-\frac{1}{720}\left(\frac{\hbar\omega}{kT}\right)^4+\cdots\right]\frac{G(\omega)}{\omega^2}d\omega. \quad (3)$$

Using the moments of the frequency spectrum defined as $\langle\omega^n\rangle=\int_0^\infty G(\omega)\omega^n d\omega$, we can write the low- and high-temperature limits as follows[1]:

low temperature: $\langle x^2\rangle_0=(h/2m)\langle\omega^{-1}\rangle$ for $T\to 0^0$K; (4)

high temperature: $\langle x^2\rangle_T=\frac{k}{m}\left[\langle\omega^{-2}\rangle T+\tfrac{1}{12}\left(\frac{h}{k}\right)^2 T^{-1}-\frac{1}{720}\left(\frac{h}{k}\right)^4\langle\omega^2\rangle T^{-3}+\cdots\right]$. (5)

Alternatively, each term in the expansion can be described in terms of an effective Debye frequency spectrum such that its nth moment $\omega_D(n)$ corresponds to the real moment $\langle\omega^n\rangle$. The $\omega_D(n)$ define weighted Debye temperatures $\Theta_D(n)$ according to

$$\Theta_D(n)=\frac{\hbar}{k}\omega_D(n)=\frac{\hbar}{k}[\tfrac{1}{3}(n+3)\langle\omega^n\rangle]^{1/n}, \quad n>-3, n\neq 0. \quad (6)$$

Housley[1] also gives a low-temperature expansion of Eq. (1) which, with Eqs. (4) and (6), yields for cubic crystals

$$-\ln(f)_h=\kappa\langle x^2\rangle_T=\frac{3R}{2k}\left\{\frac{1}{\Theta_D(-1)}+\frac{2\pi^2 m}{3M}\left[\frac{1}{\Theta_D(-3)}\right]^3 T^2+\cdots\right\}, \quad (7)$$

where $R=E_\gamma^2/2mc^2$ is the recoil energy, m is the mass of the radiating atom, and M is the total mass of the ideal unit cell. $\Theta_D(-3)$ for a pure, monatomic crystal is identical with the Debye temperature as found from low-temperature elastic constants or specific heats.[22]

From Eqs. (5) and (6) we find for high temperatures and harmonic forces

$$-\ln(f)_h=\frac{6RT}{k}\left[\frac{1}{\Theta_D(-2)}\right]^2\left\{1+\left[\frac{\Theta_D(-2)}{6T}\right]^2+\cdots\right\}. \quad (8)$$

The first term contributes more than 95% for $T/\Theta_D>0.72$.

For small cubic and quartic anharmonic contributions to the interatomic potentials and at temperatures where the second term in Eq. (8) can be neglected, Maradudin and Flinn[2] have given an anharmonic correction to f:

$$-\ln f(T)=-\ln f_h(T)[1+\epsilon(-2)T]. \quad (9)$$

The anharmonicity parameter $\epsilon(-2)$ depends on the second and higher derivatives of the interatomic potentials[2]; the theory does not take impurities into account, however. $\epsilon(-2)$ is the fractional change of the moment $\omega_D(-2)$ with temperature due to anharmonicity.[3] (See Sec. 4.3.)

We have found that an excellent fit to our data can be obtained if we use a Debye function $f_D(T,\Theta_D)$ for $f_h(T)$. In Figs. 3–5, we have plotted

$$-\ln f(T)=-[1+\epsilon(-2)T]\ln f_D(T,\Theta_D) \quad (10)$$

over a large temperature range for a proper choice of the constants $\epsilon(-2)$ and Θ_D. We have evaluated these constants, using for $f_D(T,\Theta_D)$ a table of Debye integrals,[23] by assuming a value for $\epsilon(-2)$ and calculating the corresponding Θ_D for each datum point, then varying $\epsilon(-2)$ until these values of Θ_D show a minimum standard deviation. The procedure is illustrated in Tables I–III. We have included Sprague's f values[14] in our data for Cu.

The low-temperature points for Pd and Pt have been plotted separately against T^2 [see Eq. (7)] in Figs. 6 and 7. On the same graphs, we show a best fit for both

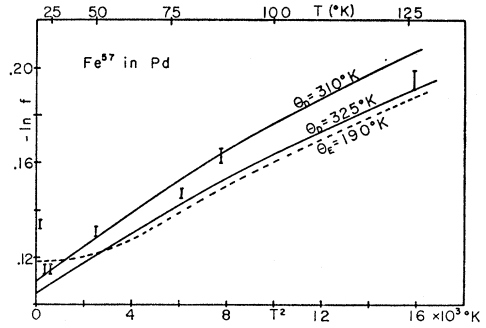

FIG. 6. Comparison of the low-temperature f values of Fe^{57} in Pd with Debye and Einstein functions. (See Sec. 4.2.)

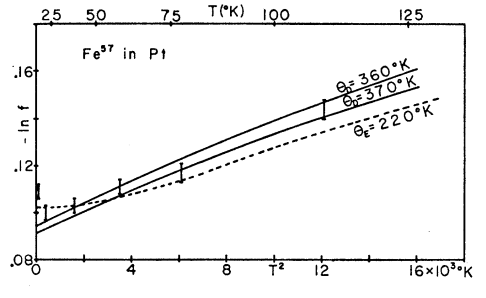

FIG. 7. Comparison of the low-temperature f values of Fe^{57} in Pt with Debye and Einstein functions. (See Sec. 4.2.)

[22] L. S. Salter, Advan. Phys. 14, 1 (1965).

[23] A. H. Muir, Atomic International Document No. AI-6699, 1962 (unpublished).

TABLE IV. Weighted Debye temperatures and anharmonicity parameters of Fe^{57} in Cu, Pd, Pt, and Ni.

	Cu	Pd	Pt	Ni[a]
$\Theta_D(-1)$ (°K)	363±7	310±10	360±10	···
$\Theta_D(-2)$ (°K)	372±3	325±3	369±3	505±10
$\epsilon(-2)$ $(10^4\ °K)^{-1}$	4.5±0.5	1.7±0.3	1.8±0.3	10±1

[a] Reference 17.

a Debye and an Einstein function (see Sec. 4.3). From the graphs, and using Eqs. (7) and (8), we obtained values of $\Theta_D(-1)$ and $\Theta_D(-2)$, respectively. Our data do not allow a meaningful determination of $\Theta_D(2)$ [Eq. (8)] or $\Theta_D(-3)$ [Eq. (7)].

3.3 Comparison between Impurity and Host Parameters

In Table IV, we summarize the values for $\Theta_D(-1)$, $\Theta_D(-2)$, and the anharmonicity parameter $\epsilon(-2)$ as derived from our f measurements. Included are also earlier data[17] on Fe in Ni for comparison in Secs. 4.1 and 4.3.

For comparison, we list in Table V corresponding data for the host materials. We postpone the detailed discussion of the anharmonicity parameters to Sec. 4.3. For Cu, the weighted Debye temperatures and the listed values for ϵ were derived from the moments of the frequency distribution $G_h(\omega)$, as obtained from inelastic-neutron-scattering data[24] at 49 and 298°K. For Pd, the only data available for comparison are $\Theta_D(-3)$ values from low-temperature specific-heat capacities and elastic constants.[25] Reasonable estimates for $\Theta_D(-1)$ and $\Theta_D(-2)$ for Pd, entered in parentheses, were obtained by observing that in two other fcc metals, Cu and Al, the ratios $\Theta_D(-1)/\Theta_D(-3)$ and $\Theta_D(-2)/\Theta_D(-3)$ are 0.91±0.01 and 0.93±0.01, respectively.[24,26] In general, these ratios for fcc metals seem to differ only by a few percent.[27] For Pt two values each have been entered in Table V for $\Theta_D(-1)$ and $\Theta_D(-2)$. We list in parentheses estimates obtained from $\Theta_D(-3)$, using the same ratios as were used for Pd. The other values listed are those obtained from an analysis of thermal data,[28] which carry rather large uncertainties. The value of $\Theta_D(-3)$ for Pt is taken from recent low-temperature heat-capacity data.[29] For Ni, all values, except one for $\Theta_D(-3)$, are placed in parentheses to indicate that they are estimates only. One pair of $\Theta_D(-2)$ and $\Theta_D(-3)$ values was taken from room-temperature neutron-scattering data.[30] The discrepancy between $\Theta_D(-3)=476$°K from low-temperature elastic constants[31] and $\Theta_D(-3)=451$°K from Ref. 30 suggests that the room-temperature moments obtained by the neutron-scattering experiments[30] are shifted because of anharmonicity, as has been found[24] for Cu. Using the estimate for the anharmonicity parameter $\epsilon(-3)$ from the two values of $\omega_D(-3)$, we entered for Ni a corrected value for $\Theta_D(-2)=423$°K. (See Sec. 4.3.)

TABLE V. Weighted Debye temperatures and anharmonicity parameters of the host materials.

		Cu	Pd	Pt	Ni
$\Theta_D(-1)$ (°K)		316[a]	(249)[e]	(215)[e] 230[f]	···
$\Theta_D(-2)$ (°K)		322[a]	(255)[e]	(219)[e] 230[f]	(423)[i] (401)[j]
$\Theta_D(-3)$ (°K)		346[a]	274[d]	236[g]	476[k] (451)[j]
Anharmonicity parameter $(10^4\ °K)^{-1}$	$\epsilon(-2)$	1.2[b]	(1.6)[e]	(1.4)[e]	(1.4)[l]
	$\epsilon(-3)$	3.3[b]	···	(1.6)[h]	3.5[m]

[a] From 49°K data, Ref. 24.
[b] Reference 24; see Sec. 4.3.
[c] Estimates from $\Theta_D(-3)$; see Sec. 3.3.
[d] Reference 25.
[e] Reference 3; see Sec. 4.3.
[f] Reference 28.
[g] Reference 29.
[h] Reference 35.
[i] Estimate from $\Theta_D(-3)=476$°K, using $\epsilon(-3)$; see Sec. 4.3.
[j] From 296°K data, Ref. 30.
[k] Low-temperature data, Ref. 31.
[l] From thermodynamic data, similar to Ref. 3; see Sec. 4.3.
[m] From comparing $\Theta_D(-3)$ at 0°K (Ref. 31) and at 296°K (Ref. 30).

4. DISCUSSION AND CONCLUSIONS

4.1 Impurity-Host Binding

Lipkin[32] has shown that for an isotopic impurity (no change in force constants) in a harmonic crystal, and assuming a reasonable frequency spectrum $G_h(\omega)$ for a real host lattice, the mean-squared displacement of the impurity atoms at $T=0$°K should be related to that of the host atoms by the square root of the mass ratio to within a few percent:

$$[\langle x^2\rangle_0]_{\text{eff}}=q^{1/2}[\langle x^2\rangle_0]_{\text{host}},\ \text{with}\ q=(m_{\text{imp}}/m_{\text{host}}),\quad (11)$$

or, from Eq. (7), Sec. 3.2,

$$[\Theta_D(-1)]_{\text{eff}}=q^{-1/2}[\Theta_D(-1)]_{\text{host}}.\quad (12)$$

A deviation from the above relation would therefore indicate a change in the impurity-to-host force constants as compared with those of the host. In the upper part of Table VI, we list the values of $[\Theta_D(-1)]_{\text{eff}}$ from Table V and Eq. (12), and the ratio $[\Theta_D(-1)]_{\text{imp}}/[\Theta_D(-1)]_{\text{eff}}$ from the data in Table IV. From these ratios it can be concluded that Fe^{57} is more strongly

[24] R. M. Nicklow, G. Gilat, H. G. Smith, L. J. Raubenheimer, and M. K. Wilkinson, Phys. Rev. **164**, 922 (1967).
[25] B. W. Veal and J. A. Rayne, Phys. Rev. **135**, A442 (1964).
[26] G. Gilat and R. M. Nicklow, Phys. Rev. **143**, 487 (1966).
[27] T. H. K. Barron, A. J. Leadbetter, J. A. Morrison, and L. S. Salter, in *Inelastic Scattering of Neutrons in Solids and Liquids* (IAEA, Vienna, 1963), Vol. I, p. 49.
[28] J. L. Feldman and G. K. Horton, Phys. Rev. **137**, A1106 (1965).
[29] G. E. Shoemake and J. A. Rayne, Phys. Letters (Netherlands) **26A**, 222 (1968).
[30] R. J. Birgeneau, J. Cordes, G. Dolling, and A. D. B. Woods, Phys. Rev. **136**, A1359 (1964).
[31] G. A. Alers and J. R. Neighbours, Rev. Mod. Phys. **31**, 675 (1959).
[32] H. J. Lipkin, Ann. Phys. (N. Y.) **23**, 28 (1963).

bound in Cu than is a Cu atom, while, on the other hand, the Fe impurity atom is less tightly bound in both the Pd and Pt crystals than is a host of atom.

A quantitative evaluation of the force-constant changes is, of course, dependent upon the assumed dynamic model for the crystal. Two simple models have been treated in the literature. Visscher[6] has assumed a substitutional impurity in a harmonic, simple cubic lattice, nearest-neighbor interactions only, and a single shear and compressional force constant α. He finds in the limit $T\rightarrow 0°$

$$[\Theta_D(-1)]_{\rm imp}=[\Theta_D(-1)]_{\rm host}q^{-1/2}[\alpha'/\alpha]^{1/2}. \quad (13)$$

The impurity-to-host force-constant ratio α'/α listed in the next-to-last line of Table VI has been calculated from our low-temperature data, using Eqs. (12) and (13):

$$\alpha'/\alpha=\{[\Theta_D(-1)]_{\rm imp}/[\Theta_D(-1)]_{\rm eff}\}^2. \quad (14)$$

Maradudin and Flinn[33] have assumed a harmonic fcc lattice with one central force constant and nearest-neighbor interactions only. For this model, the force-constant ratios can be obtained from the high-temperature data[33]:

$$[\Theta_D(-2)]_{\rm imp}=[\Theta_D(-2)]_{\rm eff}$$
$$\times\left\{1+0.60\left(\frac{\alpha-\alpha'}{\alpha}\right)+0.74\left(\frac{\alpha-\alpha'}{\alpha}\right)^2+\cdots\right\}^{-1/2}, \quad (15)$$

where $[\Theta_D(-2)]_{\rm eff}$ is defined as in Eq. (12). The resulting quadratic equation in α'/α can be solved if $(\Theta_{\rm imp}/\Theta_{\rm eff})<1.07$. For relative force-constant changes $|(\alpha-\alpha')/\alpha|>0.16$, higher terms in Eq. (15) are likely to become important. We have included α'/α from Eq. (15) in the last line of Table VI for comparison, although all of our data lie outside the aforementioned limits. The two sets of force-constant ratios agree reasonably well. The greatest force-constant change, a relative weakening of the binding, is found in Pt.

4.2 Localized Modes

The Visscher model,[6] as well as a more realistic crystal model of Lehman and DeWames,[7] predicts the existence of a localized mode for Fe in Pt for the mass and force-constant ratios found, while such a mode may also exist in Pd. A localized mode would add to $G_i(\omega)$ an Einstein-like peak above the cutoff frequency for the host lattice.[6,7] The effect of such a high-frequency contribution to $G_i(\omega)$ on the very-low-temperature behavior of $\langle x^2\rangle_T$ as predicted by Visscher's theory[6] is illustrated by the difference between the Einstein and Debye functions in Figs. 6 and 7. A comparison between these two figures suggests that the low-temperature behavior of Pt tends to fit better with a mixture of a Debye and an Einstein spectrum. The interference from magnetic splitting (see Sec. 3.1), as well as the limits of accuracy of our data, however, preclude an unambiguous interpretation. Since we found no anomalous Mössbauer line shape for our Pt source, we conclude that, if a localized mode of Fe in Pt does indeed exist, its thermal relaxation time is short compared with the 10^{-7}-sec lifetime of the 14.4-keV excited state.[5]

TABLE VI. Comparison between host and impurity data from Tables IV and V and derived force-constant changes for Fe in Cu, Pd, and Pt ($q=m_{\rm imp}/m_{\rm host}$) (see Secs. 4.1 and 4.2).

	Cu $q=0.90$	Pd $q=0.54$	Pt $q=0.29$
$\Theta_D(-1)_{\rm eff}$ (°K)	344	(339)	(400)[c] 427[d]
$\Theta_{\rm imp}/\Theta_{\rm eff}$	1.09	0.91	(0.90)[c] 0.84[d]
$\Theta_D(-2)_{\rm eff}$ (°K)	339	(347)	(407)[c] 427[d]
$\Theta_{\rm imp}/\Theta_{\rm eff}$	1.10	0.94	(0.91)[c] 0.86[d]
α'/α[a]	1.19	0.83	(0.81)[c] 0.86[d]
α'/α[b]	>1.2	≈0.8	≈(0.7)[c] ≈0.6[d]

[a] From $\Theta_D(-1)$ and Ref. 6.
[c] Using estimates (c) from Table V.
[b] From $\Theta_D(-2)$ and Ref. 33.
[d] Using data from Ref. 28.

4.3 Anharmonicity

Traditionally, the effects of the anharmonic terms in the interatomic potentials on the normal-mode frequencies ω_K are described in the quasiharmonic approximation by Grüneisen constants[34] $\gamma_k=-(\partial\ln\omega_k)/(\partial\ln V)$. In this model, the lattice modes are assumed to be temperature-dependent through volume expansion only. To allow for deviations from the Debye model, as well as for a variation of γ_k with frequency, weighted Grüneisen constants $\gamma(n)=-[\partial\ln\omega_D(n)]/(\partial\ln V)$ have been used in the analysis of thermal and elastic data.[34] Within the assumptions of the model, an average value of $\gamma(n)$ is related to thermodynamic quantities[34]: $\bar\gamma=\beta V/KC_v$, where β is the volume coefficient of thermal expansion, K the isothermal compressibility, and C_v the specific heat at constant volume. In particular, the high- and low-temperature limits of $\bar\gamma$ are $\gamma(0)$ and $\gamma(-3)$, respectively,[34] while the room-temperature $\bar\gamma$ is assumed to give an estimate of $\gamma(-2)$. However, the quasiharmonic model is not generally valid, as neutron-scattering experiments have shown.[24,26] Recent theoretical investigations[3,22] lead to the conclusions that the principal effects of cubic and quartic anharmonicity are the following: (1) The independence of the normal modes is destroyed. If the anharmonic coupling is relatively weak, however, it is possible to define "pseudo-harmonic" modes which are related to the harmonic

[33] A. A. Maradudin and P. A. Flinn, Phys. Rev. 126, 2059 (1962).

[34] T. H. K. Barron, A. J. Leadbetter, and J. A. Morrison, Proc. Roy. Soc. (London) A279, 62 (1964).

TABLE VII. Change in the lattice properties due to the presence of Fe impurities.

	Pd	Pt	Cu	Ni
α'/α	0.83[b]	0.83[c]	1.19[b]	~1.5[d]
$\epsilon'(-2)/\epsilon(-2)$	~1.1	~1.3	~3.7	3–7
$a_{\alpha\text{-Fe}}/a_{\text{host}}$[a]	0.90	0.90	0.97	1.00
da/dC[a] (Å/% imp)$\times 10^3$	−1.7	−1.0	+0.6	+1.3

[a] Reference 37.
[b] From low-temperature data, Eq. (14).
[c] Average from low-temperature data, Eq. (14).
[d] Estimate from high-temperature data, Eq. (15).

modes by complex shifts in the eigenvalues, involving real shifts in the frequencies of the normal modes, as well as phonon broadening (i.e., phonon lifetimes). (2) In addition to the volume dependence as accounted for in the quasiharmonic approximation, the frequencies also depend explicitly on temperature. The following approximate expression has been suggested by Baron[22,26] to describe the anharmonic shifts in the weighted frequency moments at temperature T, from their values at $T=0$:

$$\omega_D(n)_T=\omega_D(n)_0\{1-\gamma(n)[V(T)-V(0)]/V(0) +\tau(n)\langle\mathcal{E}\rangle\}. \quad (16)$$

The second term describes the volume dependence, while the parameter $\tau(n)$ describes the explicit anharmonic temperature dependence through the average vibration energy per normal mode $\langle\mathcal{E}\rangle$, including zero-point energy. In the quasiharmonic approximation, $\tau(n)\equiv 0$. The sign of $\tau(n)$ may be negative or positive, depending on whether the cubic or the quartic anharmonic term is dominant. Estimates for $\tau(n)$ have been obtained for some materials.[22,26] Pathak and Deo's[3] and Maradudin and Flinn's[33] anharmonicity parameter ϵ [see Eq. (9)] is related to Eq. (16) by the definition

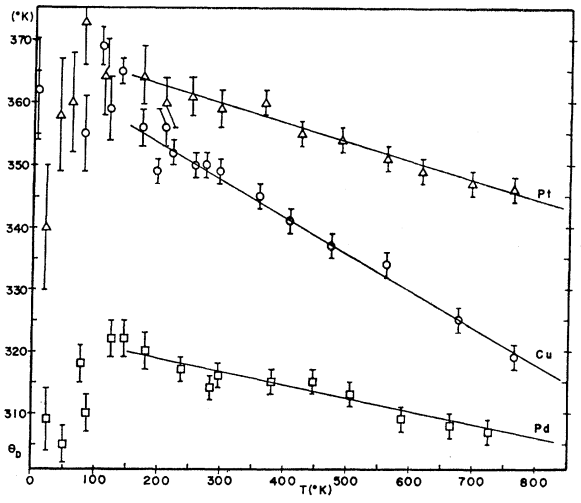

FIG. 8. Effective Debye temperatures Θ_D as a function of temperature for our three samples. No correction has been made here for anharmonicity. (See Sec. 4.3.)

$d\ln\omega_k/dT=\frac{1}{2}\epsilon_k T$, which can be generalized in analogy to Eq. (16):

$$\omega_D(n)_T=\omega_D(n)_0[1-\tfrac{1}{2}\epsilon(n)T]. \quad (17)$$

In particular, for $n=-2$ and from Eqs. (6) and (8) (in the high-temperature limit), we obtain Eq. (9). Comparing Eq. (17) with Eq. (16) for $n=-2$, we see that in the quasiharmonic approximation[3] $[\tau(-2)=0]$:

$$\gamma(-2)\Delta V/V(0)\simeq\tfrac{1}{2}\epsilon(-2)_{\text{qh}},$$

or

$$\epsilon(-2)_{\text{qh}}\simeq 2\beta\gamma(-2). \quad (18)$$

In comparing values for $\epsilon(-2)$ from our f measurements in Table IV with host data in Table V, it should be emphasized that an equivalent value for the host $\epsilon(-2)$ is directly obtainable for Cu only from[24] $\omega_D(-2)_{2\cdot 6°}/\omega_D(-2)_{49°}$. This value of 1.2×10^{-4} °K^{-1}, if compared with the quasiharmonic estimate[3] [Eq. (18)] of 2.1×10^{-4} °K^{-1}, suggests that for Cu, $\tau(-2)>0$, or that the quartic anharmonicity seems to dominate. For Pd, Pt, and Ni, the values of $\epsilon(-2)$ in Table V are the quasiharmonic estimates from Eq. (18), since phonon-frequency measurements at two temperatures are not available. For Pt, an estimate for $\epsilon(-3)_{\text{qh}}$ was also obtained from Eq. (18) for comparison. For Ni, a better value for $\epsilon(-3)$ than the quasiharmonic estimate can be obtained, if it is assumed that the low-temperature thermal constants[35] give a reliable value for $\Theta_D(-3)_0$. The room-temperature neutron-scattering data, on the other hand, yield $\Theta_D(-3)$ at 296°K. The value $\epsilon(-3)=3.5\times 10^{-4}$ °K^{-1} was obtained from these data using Eq. (17). It compares well with the corresponding value for Cu. Comparing the values of $\epsilon(-2)$ and $\epsilon(-3)$ (see Refs. 24 and 26), it appears that the relative shifts due to anharmonicity are greater for the low-frequency modes which make f measurements more sensitive to anharmonic frequency shifts than specific-heat measurements.

Keeping the above limited information on host-anharmonicity data in mind, we can draw some tentative conclusions from a comparison of Tables IV and V. Fe in Cu as well as in Ni shows an anomalously large anharmonicity parameter $\epsilon(-2)$, compared with that of the host materials, while Fe in Pd and Pt seems to show approximately the same anharmonicity as the hosts. (See Table VII.) The increased anharmonicity for Fe in Cu and Ni is apparently correlated with an increased average force constant, suggesting a local deformation around the impurity (see Table VII and and Sec. 4.4). Our value for $\epsilon(-2)$ for Fe in Cu agrees with that found by Housley *et al.*[36] for the same system.

The decrease with temperature of $\omega_D(-2)$ of the impurity response function $G_i(\omega)$ is also illustrated in Fig. 8, which gives the temperature dependence of $\Theta_D(T)$

[35] K. Andres, Phys. Letters (Netherlands) **7**, 315 (1963).
[36] R. M. Housley, F. Hess, and T. Sinnema (to be published).

without correction for anharmonicity for our samples. Above about 150°K, $\Theta_D(T) \simeq \Theta_D(-2)_T$. By comparison with Tables I–III, the importance of this correction becomes evident.

Our data do not show clear evidence for the existence of anomalous low-temperature anharmonicity as might be expected for Fe in Pd and Pt on the basis of larger atomic volumes for the host.[4]

4.4 Comparison with Other Lattice Properties

In Table VII, we summarize the various changes in lattice properties due to alloying the metals Pd, Pt, Cu, and Ni with small amounts of Fe. The first row lists the change in average force constants as discussed in Sec. 4.1 for Cu, Pd, and Pt. The force-constant ratio for Ni has been estimated from the ratio of $\Theta_D(-2)$ (see Tables IV and V), though it is well outside the limit of validity of Eq. (15). (See Sec. 4.1.)

The second row of Table VII summarizes the relative anharmonicity parameters of impurity and host atoms. (See Sec. 4.3.)

In the third row, we have shown the ratio of nearest-neighbor separation for α-Fe relative to that of the pure host.[37] We have chosen the bcc phase of α-Fe, since it has the smallest nearest-neighbor separation; all ratios in the third row would be 2.5% larger if the spacing for the fcc γ-Fe were used instead, allowing a reasonable correction for thermal expansion from 916°C, the lowest temperature at which it is stable.

In the fourth row of Table VII, we list the change in net lattice spacing[37] upon alloying each host with small amounts of Fe. In Pt and Pd, where the lattice spacing is generally larger than the "size" of the iron impurity, the change is negative, as would be expected. In Cu and Ni (and in Co and Zn as well), there is an increase in the lattice spacing in spite of the fact that the "size" is roughly the same. Moreover, adding Cu or Ni to α-Fe also increases the lattice spacing of the iron lattice. "Size" in itself does not seem to be the cause of this effect; rather, it is likely that the overlap of the d-electron wave functions is involved. Since the increased force constant and anomalously large anharmonicities seem to correlate well with increasing lattice parameters, we would also suggest that the d-electron wave functions are responsible for these effects as well.

Recent measurements[38] of the recoil-free fraction f of Fe^{57} in bcc Vanadium also indicate a rather large force-constant increase. The data have not been corrected for anharmonicity, however. The force-constant increase seems to be correlated here too with a relatively large value of $a(\alpha\text{-Fe})/a(V) = 0.95$. (See Table VII.) However, the data[37] on da/dC (Table VII) for Fe in V show the opposite (negative) sign from that of the corresponding change in lattice spacing for Fe in Cu and Ni.

Note added in proof. We regret that the room-temperature f values of Bara and Hrynkiewicz[39] were accidentally omitted from our Figs. 3–5. Within their stated uncertainties of 4–5%, their data agree with ours.

ACKNOWLEDGMENTS

This work would not have been possible without the early advice and the continuing support and encouragement from J. G. Dash at the University of Washington, who acts as permanent consultant to our research project. We gratefully acknowledge the contributions from many colleagues in the course of our investigation: R. D. Taylor for the loan of the wide absorber; D. P. Johnson and several others in the Low Temperature Physics group at the University of Washington for assistance with the operation of the He cryostat; V. O. Kostroun for measuring the low-energy spectrum of our Pt source in a calibrated Si(Li) spectrometer at the University of Oregon; W. M. Visscher, R. M. Housley, and E. A. Stern for several very helpful discussions; D. L. Sprague for allowing us to use his unpublished data; and R. M. Nicklow for sending us his data prior to publication. We are grateful for the continuing hospitality of the University of Washington Physics Department, which assisted us through all of its service facilities. We also thank J. Janacek for his invaluable help with many problems requiring the assistance of the machine shop at Portland State College.

[37] W. B. Pearson, *Handbook of Lattice Spacings and Structure of Metals and Alloys* (Pergamon Press, Ltd., London, 1957).

[38] P. D. Mannheim and A. Simopoulos, Phys. Rev. **165**, 845 (1968).

[39] T. Bara and A. Z. Hrynkiewicz, Phys. Status Solidi **15**, 205 (1966).